

# NJC

Accepted Manuscript



This is an *Accepted Manuscript*, which has been through the Royal Society of Chemistry peer review process and has been accepted for publication.

*Accepted Manuscripts* are published online shortly after acceptance, before technical editing, formatting and proof reading. Using this free service, authors can make their results available to the community, in citable form, before we publish the edited article. We will replace this *Accepted Manuscript* with the edited and formatted *Advance Article* as soon as it is available.

You can find more information about *Accepted Manuscripts* in the [Information for Authors](#).

Please note that technical editing may introduce minor changes to the text and/or graphics, which may alter content. The journal's standard [Terms & Conditions](#) and the [Ethical guidelines](#) still apply. In no event shall the Royal Society of Chemistry be held responsible for any errors or omissions in this *Accepted Manuscript* or any consequences arising from the use of any information it contains.

# **Nickel-Antimony Nanoparticles Confined in SBA-15 as a Highly Efficient Catalyst for the Hydrogenation of Nitroarenes**

**Vijaykumar S. Marakatti, Sebastian C. Peter\***

New Chemistry Unit, Jawaharlal Nehru Centre for Advanced Scientific  
Research, Jakkur, Bangalore-560064, India.

*(\*Corresponding author: sebastiancp@jncasr.ac.in. Phone: 080-22082998, Fax: 080-22082627)*

---

**Abstract**

The application of NiSb nanoparticles confined in SBA-15 is found to be highly efficient catalyst for the nitroarene reduction reactions. The NiSb/SBA-15 catalysts with different chemical composition were prepared by an adsorption-reduction method and are well characterized by XRD, N<sub>2</sub>sorption, UV-Vis, ICP-OES, SEM, TEM and EDAX. The effect of different metal concentration of Ni and Sb on the formation of NiSb alloy nanoparticles on SBA-15 was investigated. The XRD, UV and TEM images confirmed the formation of uniform NiSb nanoparticles of size 4-6 nm on the SBA-15 support. The synthesized catalysts were screened for the nitroarene reduction using NaBH<sub>4</sub>. The NiSb/SBA-15 catalyst showed excellent catalytic activity compared to NiSb nanoparticles of different particle size in p-nitrophenol reduction. The NiSb/SBA-15 catalyst showed superior catalytic activity compared to any Ni nanoparticles catalysts reported so far. The NiSb/SBA-15 catalyst showed enhanced catalytic activity towards the reduction of various nitroarenes compared to Ni/SBA-15.

Keywords: NiSb alloy; SBA-15; Catalysis; Nanoparticles; Hydrogenation.

---

## 1. Introduction

Nowadays, in the field of heterogeneous catalysis, much interest has been given to the catalysts containing two metals. Bimetallic, alloy and intermetallic compounds with nano size has attracted much attention in catalysis due to their markedly novel properties than the constituent metals and, above all, their enhanced catalytic activity, selectivity, and stability in organic reaction under study.<sup>1,2</sup> The addition of second metal Al to Fe in Al-Fe intermetallics resulted in the active site isolation and alteration of the electronic structure of Fe by chemical structure of Fe by chemical bonding, as a consequence high catalytic activity was observed for alkene hydrogenation.<sup>3</sup> Similar observations were also seen in the case of Ni-Al and Pd-Ga intermetallics for the Naphthalene and olefin hydrogenation reactions.<sup>4,5</sup> From the catalytic point of view, it is necessary to reduce the particle size of the bulk materials in their micro size down to several nanometres for increasing their surface area and number of active sites. However, nanoparticles (NPs) with such a small size are tending to aggregate to reduce their surface area as a result agglomeration of NPs may significantly deteriorate their catalytic activity.<sup>6</sup> Moreover, synthesis of uniform NPs and separation of these NPs from reaction mixture are the difficulties associated with them.<sup>7</sup>

In order to overcome the above problems, metal NPs have been immobilized on various inorganic oxide supports including silica,<sup>8</sup> zeolite,<sup>9</sup> alumina,<sup>10</sup> ceria<sup>11</sup> and titania<sup>12</sup> which improves the dispersion and catalytic activity. These NPs could be effectively stabilized by the suitable supports which hold their high surface area and catalytic activity. Among these materials, mesoporous silica is one of the most widely-used supports because of its excellent access and openness to metals with better diffusion of reactant and products.<sup>13,14</sup> The mesoporous SBA-15 is a potential candidate to support metal nanoparticles due to their narrow pore size distribution, high specific surface area, thick pore walls and large pore volume.<sup>15,16,17</sup> In literature, the NPs are introduced on mesoporous SBA-15 by

different methods such as wet impregnation,<sup>18</sup> vapour-phase grafting,<sup>19</sup> direct synthesis,<sup>20</sup> metal complex immobilisation,<sup>21</sup> and adsorption-reduction.<sup>22,23,24,25</sup> Each of these methods find their own advantage and disadvantages. The adsorption-reduction method of synthesizing alloy supported catalyst involves the co-adsorption of both metal precursors onto the amine-functionalized SBA-15 followed by the reduction with NaBH<sub>4</sub>.<sup>25</sup> This method was successful in the preparation of highly dispersed and well homogenized NPs such as Au-Pd, Au-Cu, Ag-Cu, Au-Ag systems either in alloy or intermetallic forms.<sup>22,23,24,25</sup> The loading of AuPd on SBA-15 result in the isolation of Pd atoms on the surface of SBA-15, which helps in effective chemisorptions properties towards H<sub>2</sub>, CO and O<sub>2</sub>. In case of Cu-Ag nanoparticles supported SBA-15 electron transfer from copper to silver species enhances their redox properties resulting in the high catalytic activity for oxidation of methanol to CO<sub>2</sub>. The alloying gold with copper decreases the particle size lower than the pure gold and exhibit superior performance in CO oxidation. The alloying of silver with gold enhances the thermal properties of gold nanoparticles and also controls the particle size. The dispersion of nanoparticles on the SBA-15 support provides isolated active sites and as result enhances the catalytic activity in organic transformation.

Ordered NiSb compound belongs to NiAs type of crystal structure with *P6<sub>3</sub>/mmc* space group. NiSb alloy was well studied for its interesting properties such as optical,<sup>26</sup> anti corroding,<sup>27</sup> electrical<sup>28</sup> and in fuel cells as anode material for Li- ion battery.<sup>29</sup> The alloying of Sb with another metal such as Co, Ni, Zn, In or Cu has shown enhanced application in Li- ion batteries. Similarly, intermetallic formed with catalytically active metal (Ni, Co) atom surrounded by the catalytically inactive or less active metal atom (Sb) results in the isolation of catalytic active centres, which enhance the selective interaction of reactant molecule.<sup>30,31</sup> In this regard, NiSb and CoSb intermetallic compounds showed excellent catalytic activity for the hydrogenation reaction in our previous studies.<sup>30,31</sup> However, the synthesized intermetallic

compounds (NiSb and CoSb) had a lower surface area with agglomerated particles (40-70 nm). In order to enhance their physico-chemical properties for the catalytic activity, supporting them on an inert material is an ideal choice.

Aromatic amines are important class of compounds that are used in the large industrial process for the manufacture of the dye, pharmaceuticals, agrochemicals, polymers etc.<sup>32</sup> The convenient way of synthesizing the aromatic amines is by reduction of aromatic nitro compounds through the catalytic hydride transfer reaction. P-aminophenol (p-AP) obtained by the reduction of p-nitrophenol(p-NP) is an extremely important organic compound which is widely applied in manufacturing analgesics, antipyretic drugs and photographic developers. On the hand, p-NP is a common organic pollutant in industrial and agricultural waste water.<sup>33</sup> Therefore, the conversion of p-NP to p-AP over metal nanoparticles in the presence of excess reducing agent NaBH<sub>4</sub> is an eco-friendly process. This process is also considered as a model reaction to evaluate the catalytic activity of metal nanoparticles. Various noble metal nanoparticles such as Au, Pd, Pt and Rh have been extensively studied because of their efficient catalytic activities.<sup>31,34</sup> In order to reduce the cost of noble metal catalysts, transition metal based nanoparticles or composites, such as Ni nanoparticles,<sup>35</sup> Ni/Au nanostructures,<sup>36</sup> Ni/SBA-15<sup>37</sup> and reduced graphene oxide/nickel,<sup>38</sup> have been studied for the following transformation.<sup>39</sup>

In our previous work, NiSb and CoSb intermetallic compounds were studied as an active catalyst for the hydrogenation of the p-NP to p-AP.<sup>30,31</sup> In continuation of our investigation on simple, efficient, low cost and environmentally friendly catalysts for the hydrogenation of nitroarenes, herein, we report the synthesis of NiSb alloy nanoparticles supported on SBA-15 (NiSb/SBA-15) as an efficient catalyst for the reduction of nitro compounds. NiSb/SBA-15 was synthesized by adsorption-reduction method using the amine-functionalized SBA-15 followed by the reduction. However, this technique was extensively

employed for the synthesis of transition metal based nanoparticles. In the current work an attempt has been put to synthesize for the first time a NiSb nano alloy formed by the transition metal (Ni) and non transition metal (Sb) on SBA-15. The synthesized catalysts were well characterized by the XRD, ICP-OES, SEM, TEM, N<sub>2</sub>sorption and solid UV-Vis spectroscopy. The effect of different metal concentration of Ni and Sb on the formation of NiSb/SBA-15 was investigated. The application of synthesized NiSb/SBA-15 catalyst was studied for the hydrogenation of different substituted nitroarene compounds. The chemical composition of NiSb/SBA-15 was correlated with the catalytic activity. The catalytic activities of NiSb/SBA-15 were compared with that of non supported NiSb compounds along with the literature reported catalyst. The NiSb/SBA-5 catalyst showed good recyclability and applicability has been extended to the reduction other substituted nitro aromatics.

## 2. Experimental

### 2.1. Materials

SbCl<sub>3</sub>(anhydrous, 99 %, Alfa aesar), NiCl<sub>2</sub>.6H<sub>2</sub>O(99%, SDFCL), sodium borohydride (NaBH<sub>4</sub>)(98% Sigma Aldrich), tetraethylorthosilicate (TEOS)(98%, Sigma Aldrich), 3-aminopropyl-triethoxysilane (APTES) (Sigma Aldrich) and pluronicP-123[poly(ethylene glycol)-*block*-poly(propylene glycol)-*block*-poly(ethylene glycol)], (M<sub>n</sub> ~ 5800) (Sigma Aldrich) were used for the synthesis of catalyst without further purification.

### 2.2. Synthesis

#### 2.2.1. Synthesis of SBA-15

The support SBA-15 was prepared according to the literature procedure using pluronicP-123 as template and TEOS as a silica source in an acidic medium.<sup>40</sup> In atypical procedure, 4 g of pluronic P-123 surfactant was dissolved in 20 g of water followed by the addition of 80 g of 2M HCl. To the above solution, 8 g of TEOS was added slowly and stirring was continued for next 24 hrs at 40 °C. Then, the gel mixture was transferred to a

polypropylene bottle and hydrothermally treated at 100 °C for 48 h. The solid was filtered, washed with water, and finally dried at 60 °C for 8 h. The template was removed by calcination at 550 °C (heating rate = 2 °C /min) for 6 h in presence air. The obtained porous material is designated as SBA-15.

### 2.2.2. Functionalization of SBA-15 with organosilanes

The calcined SBA-15 material was grafted with 3-aminopropyl-triethoxysilane (APTES) to functionalize the support before modification with metals.<sup>22,23,24</sup> The grafting was done by following the published procedure: 1 g of SBA-15 powder was refluxed in a ethanol solution (50 mL) containing 2.5 g of APTES for 8h. The catalyst (SBA-15-NH<sub>2</sub>) was recovered by filtration followed by washing in ethanol and acetonitrile. Finally, the amine functionalized SBA-15 was dried in an oven at 60 °C.

### 2.2.3. Modification of SBA-15-NH<sub>2</sub> with metals (Ni, Sb).

To obtain Ni-SBA-15 and Sb-SBA-15 catalysts, the functionalized SBA-15-NH<sub>2</sub> (100 mg) material was stirred for 2 h in 10 ml of ethanol solution of nickel nitrate hexahydrate (NiNO<sub>3</sub> · 6H<sub>2</sub>O = 10 wt % of Ni as assumed) or antimony chloride (SbCl<sub>3</sub> = 3 wt % of Sb as assumed) at room temperature (RT). The preparation procedure of the alloy system NiSb-SBA-15 was as follows: 10 ml of ethanol solution of antimony chloride (3 wt % of Sb as assumed) and 10 ml of ethanol solution of Ni nitrate (3 or 10 wt % of Ni as assumed) were prepared separately and mixed for 5 min in one flask. Then 100 mg of NH<sub>2</sub>-SBA-15 was added to the above solution and sonicated for a 15min followed by stirring for 2 h at room temperature.

The solid was recovered after the adsorption by filtration and washed with 50 ml of ethanol. Thus obtained solid was treated with 10 ml 0.1M NaBH<sub>4</sub> solution (prepared in ethanol) and the solution was stirred for a 2 h at 60 °C. Keeping the solution temperature at 60 °C is essential step for the reduction of Sb. The solid was filtered, dried at 100 °C and



finally calcined at 500 °C for 1 h in a static air followed by the reduction in presence of H<sub>2</sub> gas at 500 °C for 2 h.

### 2.3. Characterization of catalyst

The materials prepared were characterized using X-ray Diffraction (XRD), N<sub>2</sub> sorption, inductively coupled plasma optical emission spectroscopy (ICP-OES), scanning electron microscopy (SEM), transmission electron microscopy (TEM), energy dispersive X-ray spectroscopy (EDAX) and UV-Vis diffuse reflectance spectrometer (UV-Vis DRS). Powder XRD data were collected on a PANalytical Empyrean PXRD using CuK<sub>α</sub> radiation with scan rate of 0.187/min and 0.05/min in the wide (25-70°) and small angle (0.8-5°) range, respectively.

The N<sub>2</sub> sorption isotherms were obtained in Quanta chrome Instrument at 77 K. The surface area was calculated by BET Method, whereas the pore volume and pore diameter of mesopores were determined by the BJH method. TEM images with EDAX pattern were collected using FEI TITAN3 electron microscope operating at 80-300 kV. The samples for these measurements were prepared by sonicating the NiSb/SBA-15 powder in ethanol and drop-casting a small volume onto a carbon-coated copper grid. The FE-SEM of the synthesized catalyst was measured by the FEI Quanta 3D instrument. The samples were prepared by sonicating the powder in ethanol and drop casting a small volume on to a clean silica wafer.

UV-Vis DRS was recorded in the range of 200-800nm by a PerkinElmer LAMBDA 950 spectrophotometer with BaSO<sub>4</sub> as a blank. The amount of Ni and Sb in the synthesized catalysts was determined using ICP-OES. Samples were digested in concentrated aqua regia and hydrofluoric acid followed by dilution with distilled water. ICP-OES was carried out using Perkin-Elmer Optima 7000 DV machine.

### 2.4. Catalytic activity

In a typical nitroarene reduction, 1 mL ( $1.0 \times 10^{-4}$  M) aqueous solution of p-NP and 1 mL (500 mg/10 ml) aqueous NiSb/SBA-15 suspension were mixed together in a 1 cm quartz cuvette. Freshly prepared, 1 ml ( $6 \times 10^{-2}$  M) aqueous NaBH<sub>4</sub> solution was added to the reaction mixture and time-dependent adsorption spectra were recorded in the UV-Vis spectrophotometer at room temperature.<sup>30,31</sup> In the case of nitrobenzene and 4-chloro-nitrobenzene, the sample was prepared in the methanol and the reaction was carried out in the similar way as mentioned above.

### 3. Results and Discussion

The NiSb/SBA-15 was synthesized by adsorption-reduction method using the amine-functionalized SBA-15 followed by the reduction method and well characterized by the XRD, ICP-OES, SEM, TEM, N<sub>2</sub> sorption and solid UV-Vis spectroscopy. Thus synthesized NiSb/SBA-15 catalysts with different chemical composition were studied for the hydrogenation of different substituted nitroarene compounds.

#### 3.1 Characterization of NiSb/SBA-15 catalysts

Figs. 1 and 2 represent the low ( $2\theta = 0.8$  to  $5.0^\circ$ ) and wide angle ( $2\theta = 25$ - $70^\circ$ ) XRD data, respectively for SBA-15 and NiSb/SBA-15. The various loadings of Ni and Sb on SBA-15 are listed in Table 1. The low angle XRD pattern of SBA-15 shows three well resolved diffraction peaks i.e. very strong (100) peak at  $2\theta = 1.02^\circ$  followed by another two weak peaks at  $2\theta = 1.68^\circ$  and  $2\theta = 1.95^\circ$  correspond to the (110) and (200) planes, respectively. The presence of these planes clearly indicates the existence of ordered two-dimensional hexagonal structure in SBA-15. The  $d_{100}$  spacing of SBA-15 estimated from the low angle XRD is found to be  $\sim 8.66$  nm, which is in consistent with the TEM observation. The XRD patterns of NiSb/SBA-15 catalysts also exhibited the peaks (100), (110) and (200) with intensity lower than that of SBA-15, revealing the decrease in ordering of the mesoporous structures.

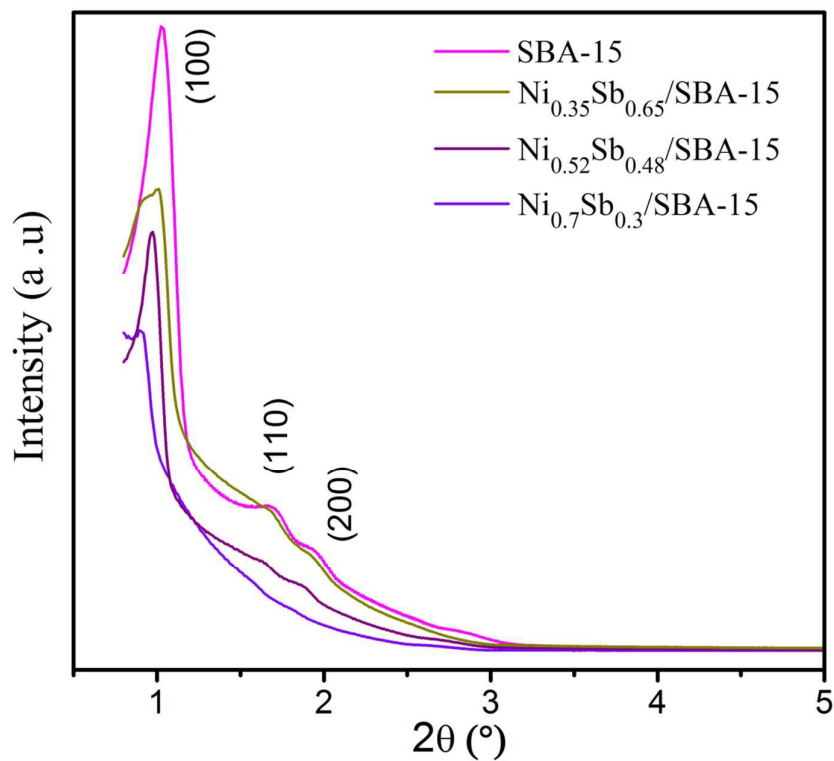


**Figure1.** Low angle ( $2\theta = 0.5-5.0^\circ$ ) XRD patterns of SBA-15 and NiSb/SBA-15 catalysts with various Ni-Sb loading.

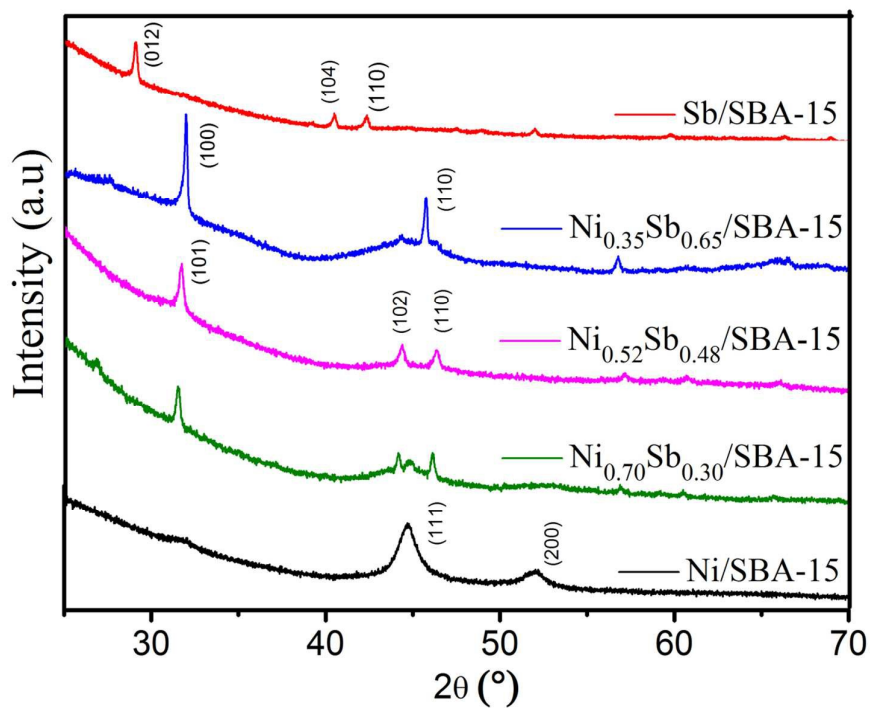


**Figure2.** Wide angle ( $2\theta = 25-70^\circ$ ) XRD patterns of NiSb and NiSb/SBA-15 catalysts with various Ni-Sb loading.

In order to synthesize NiSb NPs on SBA-15, at the beginning, we have prepared the compound using equivalent concentration (3 wt %) of Ni and Sb solution. Interestingly, the XRD pattern of thus synthesized compound showed the formation of only Sb incorporated phase, indicating more affinity of Sb to amine functionalized SBA-15 than Ni. In order to incorporate Ni into the SBA-15, nickel concentration has to be varied from 5 to 10 wt % keeping the Sb concentration constant (3 wt%) as shown in Table 1. The increase of Ni concentration from 3 to 5 wt% resulted in the formation of NiSb solid solution with the chemical composition of Ni:Sb = 0.35:0.65 as determined by the ICP-OES analysis and XRD (Table 1 and Fig. 2). The powder XRD pattern of Ni<sub>0.35</sub>Sb<sub>0.65</sub>/SBA-15 matches with the XRD pattern of Ni<sub>0.15</sub>Sb<sub>0.85</sub> solid solution with a shift in the 2θ value at higher angle can be attributed to the excess amount of Ni in the former than the latter (Fig. S1). Further increase of Ni concentration to 7.5 wt% resulted in the formation of NiSb alloy having chemical

**Table 1.** Physico-chemical properties of SBA-15, Sb/SBA-15, Ni/SBA-15 and NiSb/SBA-15 catalysts.

Catalyst Chemical composition	Nominal Loading <sup>a</sup>		Actual Loading <sup>b</sup>		Total loading (wt %)	Surface Area (m <sup>2</sup> /g)	Pore Volume (cc/g)	Average Pore diameter (nm)
	(wt %)		(wt %)					
	Ni	Sb	Ni	Sb				
SBA-15	--	--	--	--	--	589	0.717	6.63
Sb/SBA-15	--	3	--	2.85	2.8	--	--	--
Ni <sub>0.35</sub> Sb <sub>0.65</sub> /SBA-15	5	3	1.54	2.79	4.3	462	0.681	6.50
Ni <sub>0.52</sub> Sb <sub>0.48</sub> /SBA-15	7.5	3	2.84	2.59	5.4	416	0.645	5.92
Ni <sub>0.70</sub> Sb <sub>0.30</sub> /SBA-15	10	3	3.31	1.47	4.8	426	0.648	5.93
Ni/SBA-15	10	--	4.80	--	4.8	--	---	--

<sup>a</sup>Initial concentration for the ion exchange    <sup>b</sup>Determined by ICP (Standard Deviation = ± 0.1)

composition Ni:Sb = 0.52:0.48. The comparison of Ni<sub>0.52</sub>Sb<sub>0.48</sub> phase with the NiSb alloy shows the presence of all the diffraction peaks due to the (101), (102), (110), (201) and (103) planes (Fig. S1). It could be noted that, even at the higher concentration of Ni (7.5 wt %), the

amount of adsorbed Sb (2.6~2.8 wt %) on SBA-15 was the same. At still higher concentration of Ni (10 wt%), the adsorption of Sb on SBA-15 decreased with the formation of NiSb alloy ( $\text{Ni}_{0.7}\text{Sb}_{0.3}/\text{SBA-15}$ ) along with the presence of isolated Ni particles as determined by the XRD pattern (Fig. S2). If all Sb in this compound forms an alloy with Ni in the ratio 1:1, the amount of monometallic Ni present on SBA-15 would be around 1.8 wt%. The above results clearly specify, for the formation of NiSb/SBA-15, the concentration of Ni and Sb taken for the ion exchange was crucial in determining the formation of alloy, solid solution or monometallic. Similar kind of effect of metal concentration was reported for the adsorption of Cu and Ag on SBA-15.<sup>24</sup> For the synthesis of  $\text{Ni}_{0.52}\text{Sb}_{0.48}$  alloy supported on SBA-15 requires around 2.5 times more amount of Ni than the Sb for the adsorption. The formation of monometallic Ni/SBA-15 and Sb/SBA-15 were confirmed by comparing the XRD pattern with the simulated XRD pattern of Ni ( $Fm\bar{3}m$  space group) and Sb ( $R\bar{3}mh$  space group) as shown in Fig.S3.

$\text{N}_2$  adsorption-desorption isotherms were obtained for the calcined mesoporous SBA-15 and NiSb/SBA-15 catalysts as shown in Fig.3. The isotherm exhibits the sharp capillary condensation at high relative pressure ( $0.6 < P/P_0 < 0.8$ ) region and H1 hysteresis loop for all the catalysts. This clearly indicates the 2D hexagonal symmetry of the mesoporous materials with large pore diameter and narrow ranges of size. The BET specific surface area of calcined SBA-15 was found to be  $589 \text{ m}^2/\text{g}$ . The loading of NiSb/SBA-15 decreased the surface area, pore volume which could be due to the confined NiSb nanoparticles inside and on the SBA-15 (Table1). Fig.4 shows the pore size distribution of SBA-15 and NiSb/SBA-15 catalysts, determined by the classical BJH (Barrett–Joyner–Halenda) method. The pore diameter of

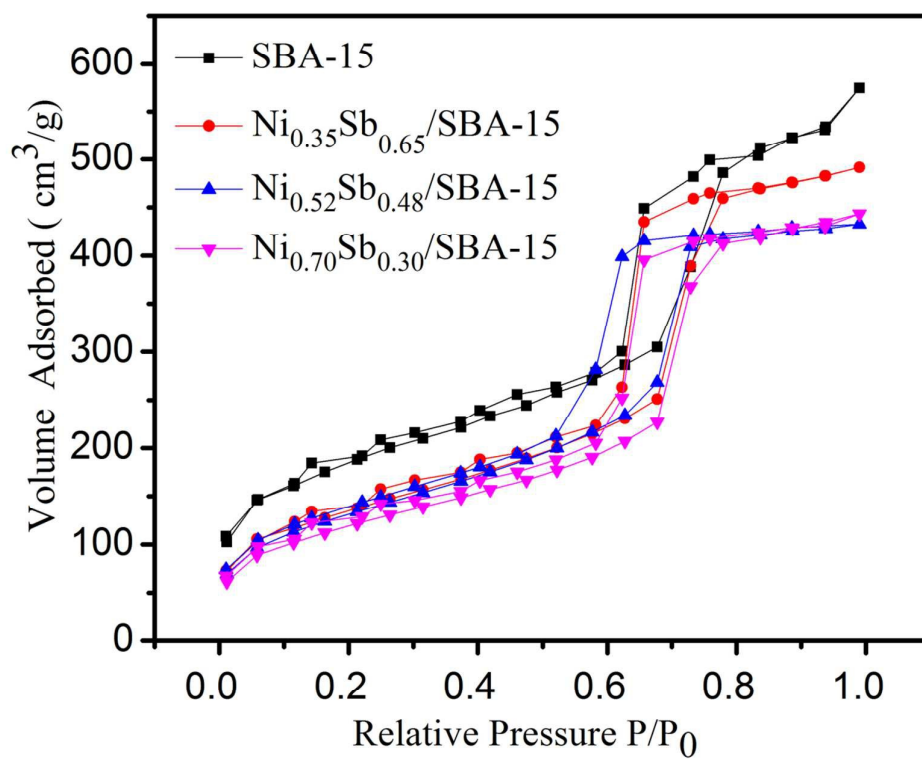


Figure3. N<sub>2</sub> adsorption isotherms for SBA-15 and NiSb/SBA-15 catalysts.

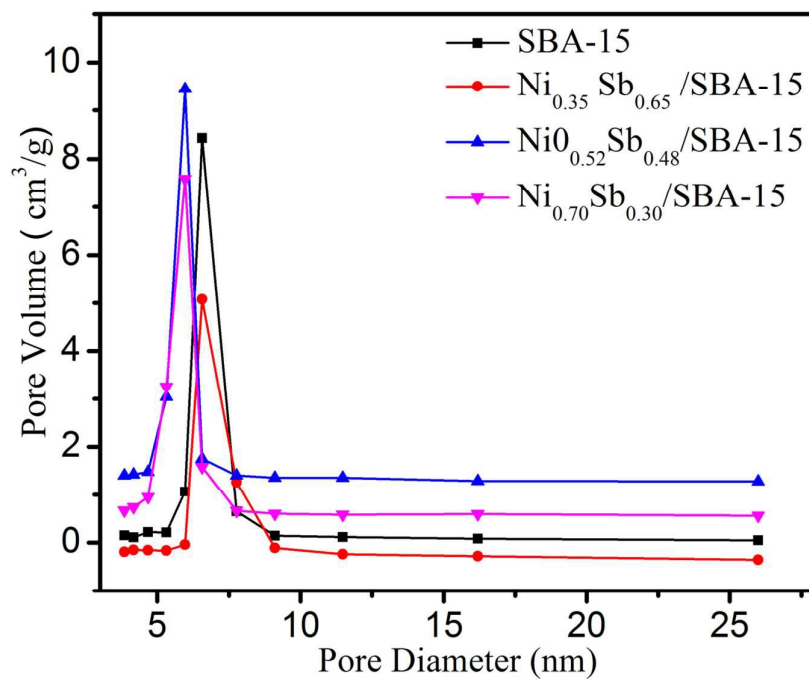
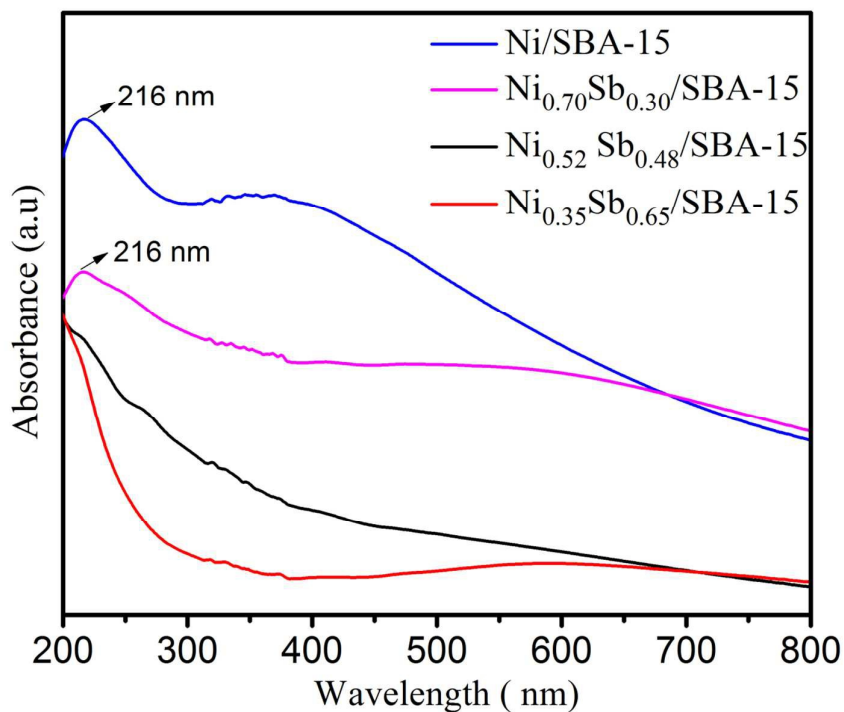


Figure4. Pore size distribution curve for SBA-15 and NiSb/SBA-15 catalysts.

SBA-15 determined by  $N_2$  sorption measurements (6.6 nm) is well supported by the pore diameter calculated by TEM measurements (8.5 nm). The pore diameter decreased slightly with of NiSb loading as compared to the SBA-15, which could be due to the presence of NiSb nanoparticles on the pore mouth and inside the pores of SBA-15

Diffuse reflectance spectroscopy is well known method for the identification and characterization of metal nanoparticles present on the supported catalysts. The UV-Vis spectra of NiSb/SBA-15 catalysts having different chemical composition are shown in Fig. 5. The monometallic Ni supported SBA-15 exhibited an absorbance band at 216 nm as reported elsewhere.<sup>16</sup>  $Ni_{0.70}Sb_{0.30}/SBA-15$  shows similar band to that of Ni/SBA-15 indicating the presence of monometallic Ni nanoparticles on SBA-15 as supported by the XRD. However,  $Ni_{0.35}Sb_{0.65}$  and  $Ni_{0.52}Sb_{0.48}$  supported on SBA-15 were found to be inactive for the UV-Vis in the absorbance region of 200 to 800 nm. This may be due the quenching effect of Sb present in the system.



**Figure 5.** DRS-UV-Vis spectroscopy of NiSb/SBA-15 catalysts

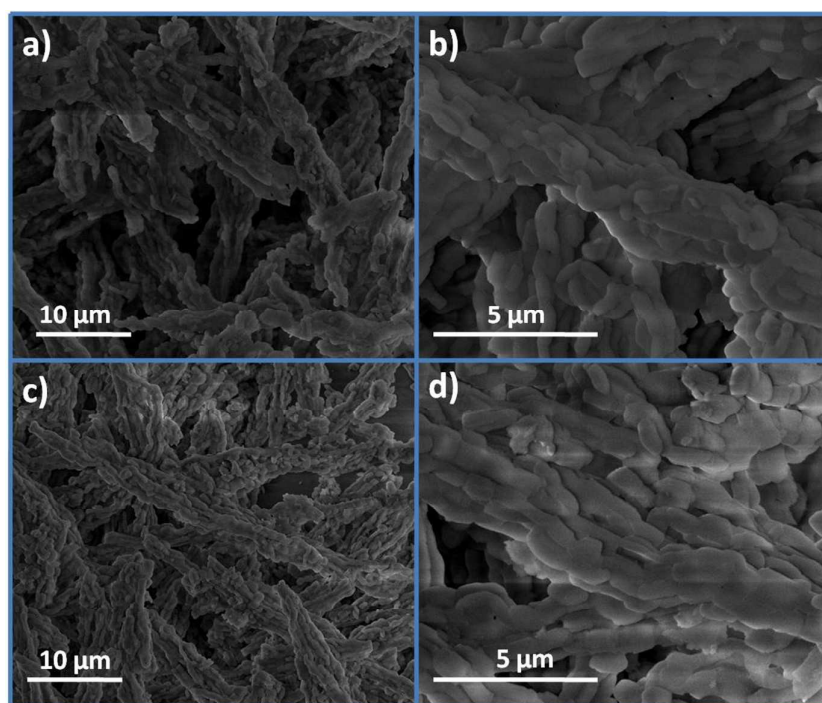


**Figure 6.** Scanning Electron Microscope (SEM) images of SBA-15(a and b) and  $\text{Ni}_{0.52}\text{Sb}_{0.48}/\text{SBA-15}$  (c and d) showing rope-like domains with wheat like macrostructures.

To study the morphology of SBA-15 before and after loading of NiSb nanoparticles, FE-SEM images were collected and shown in the Fig.6. The SEM images reveal SBA-15 consists of rope-like domains with relatively uniform sizes of  $1\ \mu\text{m}$ , which are aggregated into wheat-like macrostructures. The morphology of  $\text{Ni}_{0.52}\text{Sb}_{0.48}/\text{SBA-15}$  remained the same even after the incorporation of NiSb nanoparticles, indicating high thermal stability of the catalyst.

To study the distribution and location of NiSb particles on SBA-15, TEM images of SBA-15 and  $\text{Ni}_{0.52}\text{Sb}_{0.48}/\text{SBA-15}$  were collected. Fig.S4 represents the TEM micrograph of SBA-15 that was collected by aligning the electron beam along parallel and vertical to the primary axes of the mesopore. The average pore size of SBA-15 was found to be around  $\sim 8.5$  nm with well ordered hexagonal pores, which is consistent with the XRD data. The TEM images of  $\text{Ni}_{0.52}\text{Sb}_{0.48}/\text{SBA-15}$  along with the particle histogram are shown in Fig.7 (a-d).



The black spherical spots on the surface of SBA-15 are the NiSb nanoparticles, as supported by the EDAX and XRD patterns. The EDAX measurements on TEM images showed the chemical composition of Ni:Sb in the ratio of 57:42, which is in good agreement with the ICP analysis(Fig.S5). The average particle sizes of NiSb calculated by measuring 50 particles were found to be in the range of 4-6 nm. This clearly indicate that most of the particles were smaller than the pore sizes of SBA-15 (~8.5 nm)and are well confined inside the pore of SBA-15.The larger particles were also observed on the surface of the SBA-15 pores.Fig.7d shows the existence of NiSb nanoparticles at the pore mouth (pore openings) of SBA-15. This clearly indicates that distributions of NiSb particles on SBA-15 is uniform and are well separated. It should be pointed out that these very small NiSb alloy particles were obtained by calcining at high temperature of 500 °C in air and H<sub>2</sub>, demonstrating the formed nanoparticles are very stable and highly resistant to sintering.

### 3.2. Catalytic reduction of Nitroarenes

Catalytic test of the as synthesized catalysts were performed for the reduction of nitroarenes, especially in the conversion of p-NP to p-AP by NaBH<sub>4</sub> in aqueous phase and monitored through UV-Vis spectrophotometer. p-NP in aqueous phase exists as nitro phenolate ion with absorbance maximum ( $\lambda_{\text{max}}$ ) at 317 nm; however the addition of NaBH<sub>4</sub> enhances the basic condition of the solution as result absorbance maximum ( $\lambda_{\text{max}}$ ) shifts to 400 nm which can be observed by change in colour of solution to yellow.<sup>30,31</sup> The addition of the catalyst gradually decreased the intensity of peak at 400 nm due to the reduction of p-NP and a new peak is appears at 300 nm corresponds to the p-AP. Since the peak at 400 nm is much stronger than the peak at 300 nm, the concentration of p-NP was measured, and the kinetics of the reaction was monitored by recording the absorbance at 400 nm.

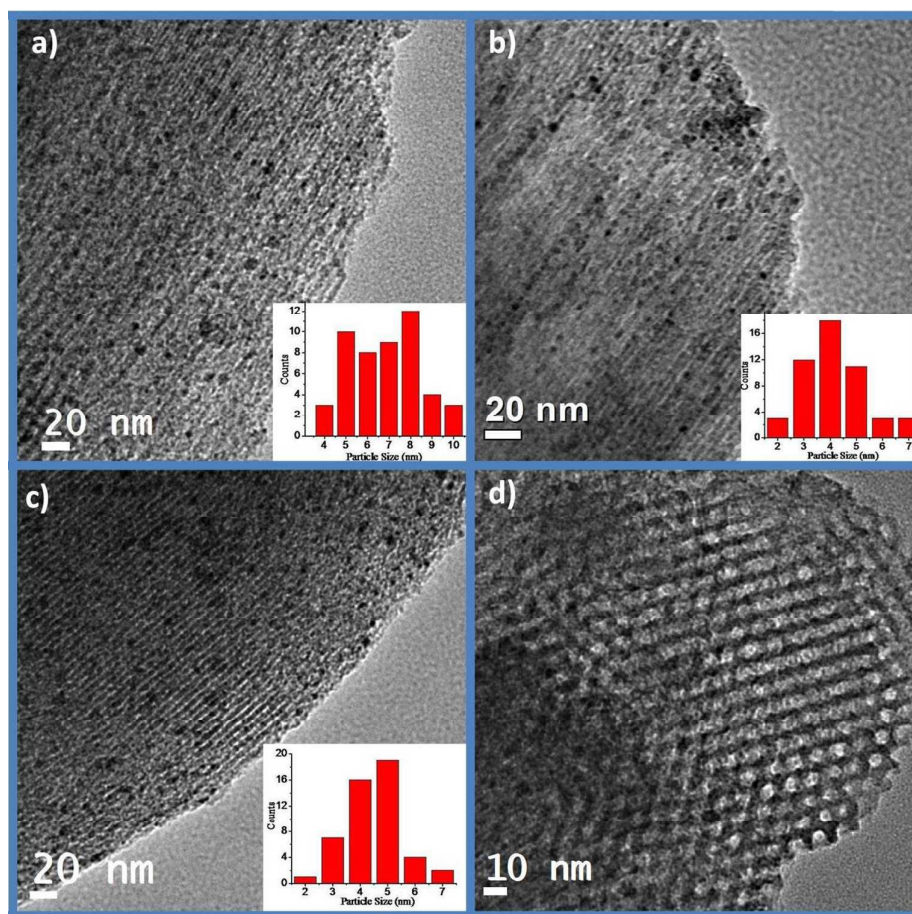


**Figure 7.** Transmission Electron Microscopy(TEM) images of Ni<sub>0.52</sub>Sb<sub>0.48</sub>/SBA-15 showing hexagonal mesopores with black NiSb particles supported on the surface(a, b and c) and at the pore mouth(d).

The p-NP reduction could not proceed in the absence of catalyst due to the kinetic barrier. The SBA-15 and amine functionalized catalyst (SBA-15-NH<sub>2</sub>) did not show any catalytic activity in the p-NP reduction, however supporting NiSb on SBA-15 subsequently increased the catalytic activity. The catalyst Ni<sub>0.52</sub>Sb<sub>0.48</sub>/SBA-15 showed complete reduction of p-NP within 10 min, whereas Ni<sub>0.35</sub>Sb<sub>0.65</sub>/SBA-15 exhibited very low catalytic activity and reaction did not complete even after 30 min(Fig.8-9).Ni<sub>0.70</sub>Sb<sub>0.30</sub>/SBA-15 and Ni/SBA-15 showed almost complete conversion of p-NP after 23 and 30 minutes, respectively (Fig.8-9).Sb/SBA-15 was found to be inactive in the reaction(Fig.S6).The reduction rate of p-NP is independent of the concentration of NaBH<sub>4</sub>, as the reaction is spontaneous and the initial

concentration of the  $\text{NaBH}_4$  is very high, which can be considered as constant throughout the reaction. Therefore, this pseudo-first-order kinetic equation is applied to evaluate the catalytic rate using the formula  $[A_t] = [A_0]e^{-Kt}$ , where  $A_t$  is absorbance at time  $t$ , represents the corresponding concentration of the reactant,  $A_0$  is the initial concentration of the reactant and  $K$  is pseudo first order rate constant.<sup>30,31</sup> The plot  $\ln(A_t/A_0)$  versus reaction time exhibits linear correlation with the reaction time, and the rate constant ( $K$ ) was calculated for all the NiSb/SBA-15 catalysts. Among the different NiSb catalysts,  $\text{Ni}_{0.52}\text{Sb}_{0.48}$ /SBA-15 catalyst showed the largest rate constant ( $3.78 \times 10^{-3}/\text{s}$ ) compared to the  $\text{Ni}_{0.35}\text{Sb}_{0.65}$ /SBA-15 and  $\text{Ni}_{0.7}\text{Sb}_{0.3}$ /SBA-15 as shown in Fig. 8.

The lower rate constant of  $\text{Ni}_{0.35}\text{Sb}_{0.65}$ /SBA-15 ( $0.66 \times 10^{-3}/\text{s}$ ) catalyst could be due to the presence of solid solution phase with less amount of Ni arranged in disordered lattice. The lower catalytic rate of  $\text{Ni}_{0.7}\text{Sb}_{0.3}$ /SBA-15 ( $1.46 \times 10^{-3}/\text{s}$ ) might be due to the presence of lower NiSb loading (3 wt %) and the presence of monometallic Ni (1.8 wt%). The catalytic rate constant for monometallic Ni/SBA-15 was found to be around  $1.0 \times 10^{-3}/\text{s}$ . The high catalytic activity in case of  $\text{Ni}_{0.52}\text{Sb}_{0.42}$ /SBA-15 can be explained by the antimony deficiency sites in NiSb. The peak corresponds to the (101) plane in the powder XRD data of  $\text{Ni}_{0.52}\text{Sb}_{0.48}$ /SBA-15 has shifted towards the higher two theta value compared to the simulated NiSb, which could be due to the deficiency of Sb (Fig. S7). The antimony deficiency was further confirmed by the compositions  $\text{Ni}_{0.52}\text{Sb}_{0.42}$  by ICP-OES and EDAX. The deficiency of the catalytically inactive Sb atom facilitates more reactant molecule to interact with the catalytically active Ni atom, retaining the surface area the same and without affecting the stability of the material. In our previous studies, we synthesized nano NiSb intermetallics with different particle size by polyol and solvothermal method.<sup>30,31</sup> The presence of these optimum amount of Sb in NiSb isolate the Ni sites for the reactant molecules, resulting high catalytic activity. As explained earlier, the possible reaction mechanism for the conversion of

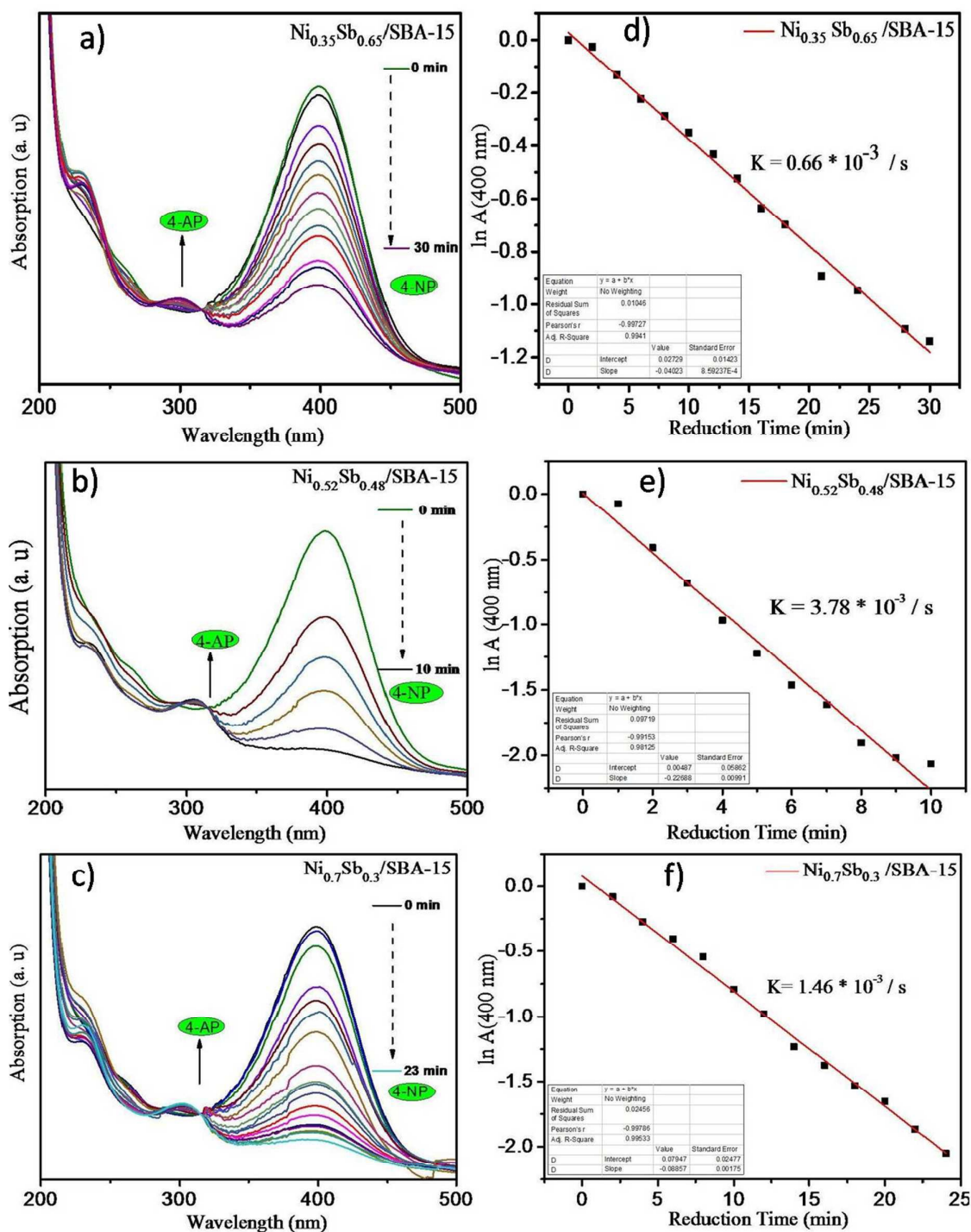


**Figure 8.** UV-Vis absorption spectra and plot of  $\ln A$  of p-NP at 400 nm vs. reduction time for the reduction of p-NP to p-AP by  $\text{Ni}_{0.35}\text{Sb}_{0.65}\text{Sb}/\text{SBA-15}$  (a and d),  $\text{Ni}_{0.52}\text{Sb}_{0.48}\text{Sb}/\text{SBA-15}$  (b and e) and  $\text{Ni}_{0.70}\text{Sb}_{0.30}\text{Sb}/\text{SBA-15}$  (c and f).

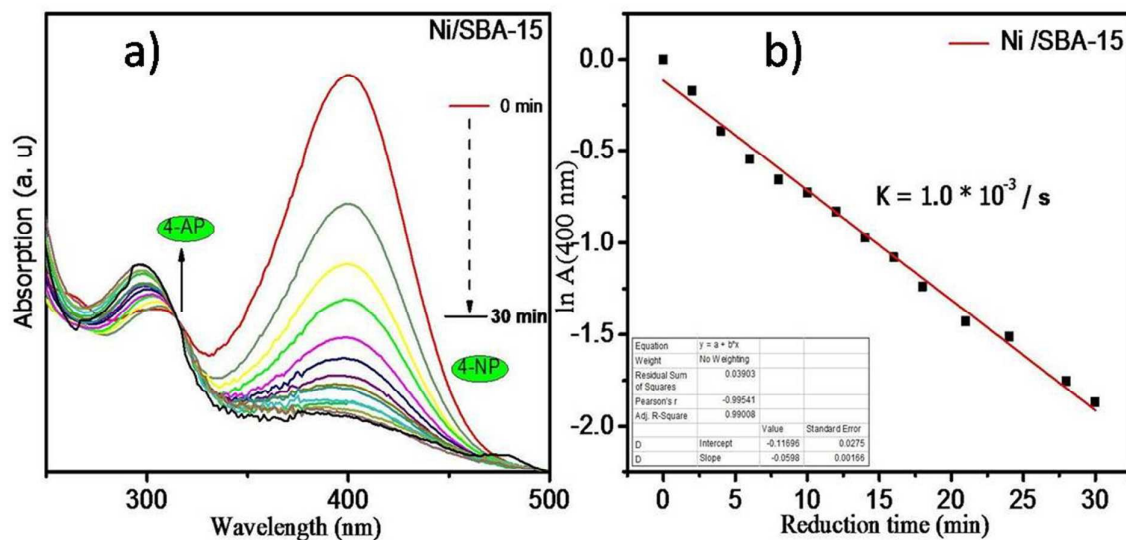


**Figure 9.** (a) UV-Vis absorption spectra and (b) plot of  $\ln A$  of p-NP at 400 nm vs. reduction time for the reduction of p-NP to p-AP by Ni/SBA-15 catalyst.

p-NP to p-AP by NiSb/SBA-15 involves the formation of active metal-hydride bond initially, followed by the adsorption of substrate (p-NP) on to the catalyst by diffusion. Finally the hydride ion transfer on to the p-NP molecule followed by product desorption from the catalyst surface with the formation of p-AP. The comparisons of the catalytic activity of these catalysts with NiSb/SBA-15 catalyst are tabulated in Table 2. The NiSb with larger particle size (40-70 nm) showed lower rate constant of  $1.53 \times 10^{-3}/s$  compared with smaller particle size of 6-15 nm, which exhibited rate constant of  $3.6 \times 10^{-3}/s$ . The NiSb particles with smallest particle size (4-6 nm) with uniformly supported on the SBA-15 showed the high rate constant of  $3.78 \times 10^{-3}/s$ . However, it is not appropriate to compare different catalysts on the basis of rate constant as it is affected by the catalyst concentration directly. Therefore, the parameter  $k$ , which is the ratio of the rate constant  $K$  to the total amount of active catalyst (NiSb) was introduced to evaluate the catalytic performance of different catalysts as listed in Table 2.

**Table 2.** Comparison of catalytic performance of NiSb/SBA-15 catalysts with other Ni and Co related catalysts for the p-NP reduction.

Catalysts	Particle size ( nm)	Rate Constant (K) (x 10 <sup>-3</sup> / s )	k <sup>a</sup> (/sg)
Ni <sub>0.35</sub> Sb <sub>0.65</sub> /SBA-15	4-6	0.66	30.7
Ni <sub>0.52</sub> Sb <sub>0.48</sub> /SBA-15	4-6	3.78	140.0
Ni <sub>0.70</sub> Sb <sub>0.30</sub> /SBA-15	4-6	1.46	60.8
Ni/SBA-15	-	1.00	41.6
<sup>b</sup> NiSb (polyol)	6-15	3.60	36.0
<sup>b</sup> NiSb (Solvothrmal)	40-70	1.53	15.3
<sup>b</sup> CoSb	6-15	1.81	18.1

<sup>a</sup>k is rate constant calculated per gram of NiSb

<sup>b</sup>Values were taken from Ref [30]

The comparison in Table 2 clearly indicates that the assynthesized Ni<sub>0.52</sub>Sb<sub>0.48</sub>/SBA-15 catalyst exhibits the high catalytic activity (k = 140/sg) compared to the unsupported NiSb catalyst, indicating the role of support in enhancement of catalytic activity. This can be understood from the particle size and structural parameters, as the particle size decreases the surface to volume ratio and energy increases which enhances the redox reaction. The particles in case of NiSb synthesized by the polyol(6-15 nm) and solvothrmal(40-70 nm) methods are agglomerated, whereas NiSb in NiSb/SBA-15 are well distributed with high active surface sites exposed to the reactant. Since, the support is inactive in the catalysis, can alter the adsorption properties of reactant and products in the reaction.<sup>41</sup> The changes in the chemisorptions strengths of reactants cause a variation in activity and selectivity in catalytic reactions, which directly influences the kinetic parameter of reaction.<sup>42</sup> The origin of this compensation effect is not unique to catalysis and similar phenomena have been observed in

a variety of different supported catalysts.<sup>41</sup>The high catalytic activity for the Ni<sub>0.52</sub>Sb<sub>0.48</sub>/SBA-15 supported catalyst could also be due to the well dispersed nanoparticles on the surface and inside the pores of SBA-15, which effectively increases the adsorption of reactant on the active sites and easy diffusion of products.<sup>36</sup>Similar kind of high catalytic activity was observed for the Ni/SBA-15 recently by Pan et al.<sup>36</sup>Table 3 shows the comparison of Ni<sub>0.52</sub>Sb<sub>0.48</sub>/SBA-15 catalyst with other reported Ni containing catalyst for the catalytic activity of p-nitrophenol reduction and NiSb/SBA-15 was found to be an outstanding catalyst with higher value of k.<sup>43,44</sup>

To study the recyclability of the Ni<sub>0.52</sub>Sb<sub>0.48</sub>/SBA-15 catalyst, after the complete conversion of first cycle, 1 ml of p-NP solution and NaBH<sub>4</sub> solution was introduced to the old reaction mixture. There was a minute increase in the reduction time observed from the

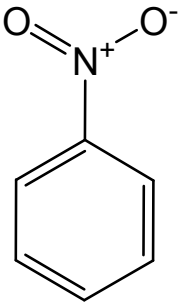
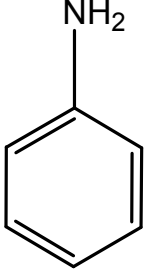
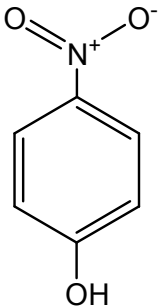
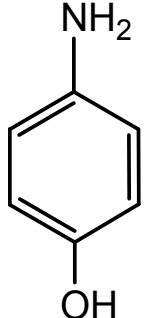
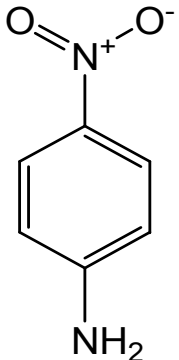
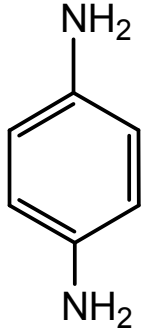
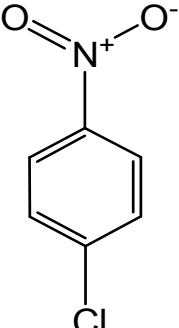
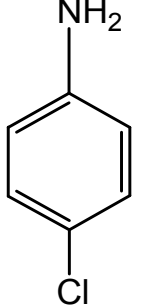
**Table 3.** Comparison of NiSb/SBA-15 catalyst with other reported catalysts.

Catalysts	Type	Rate Constant (K) (x 10 <sup>-3</sup> /s)	k <sup>a</sup> (/s g)	References
RGO/Ni	Nanocomposite	14.8	4.5	38
Ni@SiO <sub>2</sub>	Nanoparticles	2.8	0.9	39
Ni	Nanoparticles	2.4	0.8	43
RANEY ®Ni	Nanoparticles	0.3	0.1	43
Ni	Prickly structure	0.7	1.4	43
PVPh-Ni <sub>3</sub> Co	Alloy nanochain	24.1	19.0	44
Ni/SBA-15	Nanocomposite	3.0	30.0	37
Ni/SBA-15	Nanocomposite	1.0	40.0	Present work
Ni <sub>0.52</sub> Sb <sub>0.48</sub> /SBA-15	Nanocomposite	3.7	6.3 <sup>a</sup>	Present work
Ni <sub>0.52</sub> Sb <sub>0.48</sub> /SBA-15	Nanocomposite	3.7	140.0 <sup>b</sup>	Present work

<sup>a</sup>Calculated per gram of catalyst <sup>b</sup>calculated per gram of active NiSb loading.

recyclability reaction compared with the initial run, which could be due to the presence of excess of products in the reaction mixture. The rate constant for the recycled was found to be 2.33 x 10<sup>-3</sup>/s (Fig. S8).

**Table 4.** Catalytic activity comparison of Ni/SBA-15 and NiSb/SBA-15 catalyst on the reduction of different nitroarenes.

Substrate	Product	Catalyst	Reaction Time (min)	Rate Constant ( $10^{-3} \times \text{s}^{-1}$ )
		Ni <sub>0.35</sub> Sb <sub>0.65</sub> /SBA-15	24	0.14
		Ni <sub>0.52</sub> Sb <sub>0.48</sub> /SBA-15	12	0.23
		Ni <sub>0.70</sub> Sb <sub>0.30</sub> /SBA-15	24	0.11
		Ni/SBA-15	20	0.68
		Ni <sub>0.35</sub> Sb <sub>0.65</sub> /SBA-15	30	0.66
		Ni <sub>0.52</sub> Sb <sub>0.48</sub> /SBA-15	10	3.78
		Ni <sub>0.70</sub> Sb <sub>0.30</sub> /SBA-15	23	1.46
		Ni/SBA-15	30	1.00
		Ni <sub>0.35</sub> Sb <sub>0.65</sub> /SBA-15	20	0.34
		Ni <sub>0.52</sub> Sb <sub>0.48</sub> /SBA-15	08	2.40
		Ni <sub>0.70</sub> Sb <sub>0.30</sub> /SBA-15	12	1.43
		Ni/SBA-15	12	1.30
		Ni <sub>0.35</sub> Sb <sub>0.65</sub> /SBA-15	21	0.96
		Ni <sub>0.52</sub> Sb <sub>0.48</sub> /SBA-15	09	1.78
		Ni <sub>0.70</sub> Sb <sub>0.30</sub> /SBA-15	13	1.40
		Ni/SBA-15	15	1.66



To gain more insight into the scope and limitations of NiSb/SBA-15 catalyst for nitro group reduction, reactions were conducted with different types of nitro-arenes such as p-chloronitrobenzene, p-aminophenol, p-nitroaniline and nitrobenzene.(Table 4) The reaction time and rate constant of the reactions measured for the different NiSb/SBA-15 are tabulated in Table4 and respective UV-Vis absorption spectra and kinetics of the reaction are given in the supporting information (Fig. S9-14). The Ni<sub>0.52</sub>Sb<sub>0.48</sub>/SBA-15 catalyst showed high rate constant compared to other counter parts, indicating the high efficiency of the catalyst in nitroarene reduction.

#### 4. Conclusions

Application of NiSb/SBA-15 as highly efficient and reusable catalyst for the synthesis of aromatic amines from nitroarenes using NaBH<sub>4</sub> as reducing agent has been studied. We have for the first time synthesized NiSb/SBA-15 catalysts with high surface area with uniform particle size by a novel ion-exchange-reduction strategy. The investigation of different concentration of Ni and Sb on the formation of NiSb alloy nanoparticles on SBA-15 was studied and found that, for the synthesis of NiSb/SBA-15 requires around 2.5 times more amount of Ni than the Sb for the ion exchange. BET Surface area measurements on NiSb/SBA-15 catalysts exhibited H1 type hysteresis indicating the presence of well ordered mesopores. The N<sub>2</sub> sorption measurements and TEM images further confirmed the formation of uniform NiSb nano particles of size 4-6 nm inside and outside the pores of the SBA-15 support. The NiSb/SBA-15 sample exhibits excellent catalytic performance compared to unsupported NiSb nanoparticles and other reported Ni containing catalyst in the nitro arene reduction. The as-prepared NiSb/SBA-15 catalyst exhibits several advantages such as high catalytic performance, easy reuse and low cost.

## Acknowledgement

We thank Jawaharlal Nehru Centre for Advanced Scientific Research, Department of Science and Technology (DST), Council of Scientific and Industrial Research (CSIR) and sheikh saqr laboratory for financial support. S. C. P. thanks the DST for the Ramanujan fellowship (Grant SR/S2/RJN-24/2010) and V. M. thanks CSIR for the post doctoral fellowship (Grant 01(2787)/14/EMR-11). We are grateful to Prof. C. N. R. Rao for his constant support and encouragement.

## References

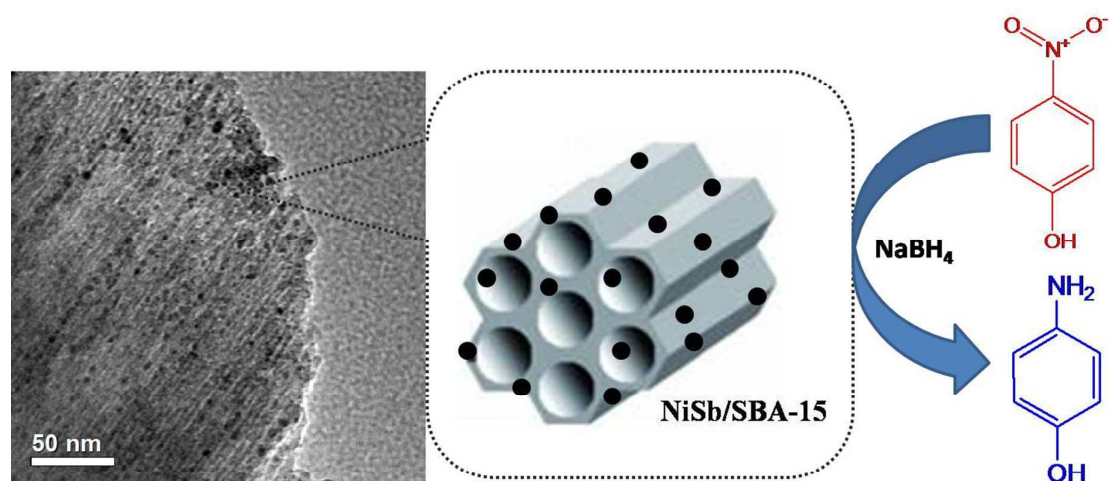
1. J. C. Bauer, X. Chen, Q. Liu, T.-H. Phan and R. E. Schaak, *J. Mater. Chem.*, 2008, **18**, 275-282.
2. M. Sankar, N. Dimitratos, P. J. Miedziak, P. P. Wells, C. J. Kiely and G. J. Hutchings, *Chem. Soc. Rev.*, 2012, **41**, 8099-8139.
3. M. Armbruster, K. Kovnir, M. Friedrich, D. Teschner, G. Wowsnick, M. Hahne, P. Gille, L. Szentmiklosi, M. Feuerbacher, M. Heggen, F. Girgsdies, D. Rosenthal, R. Schlogl and Y. Grin, *Nat. Mater.*, 2012, **11**, 690-693.
4. M. Armbruster, K. Kovnir, M. Behrens, D. Teschner, Y. Grin and R. Schlogl, *J. Am. Chem. Soc.*, 2010, **132**, 14745-14747.
5. X. Chen, Y. Ma, L. Wang, Z. H. Yang, S. H. Jin, L. L. Zhang and C. H. Liang, *Chemcatchem*, 2015, **7**, 978-983.
6. A. Roucoux, J. Schulz and H. Patin, *Chem. Rev.*, 2002, **102**, 3757-3778.
7. O. Akbulut, C. R. Mace, R. V. Martinez, A. A. Kumar, Z. H. Nie, M. R. Patton and G. M. Whitesides, *Nano Lett.*, 2012, **12**, 4060-4064.
8. W. N. Wang, Z. Meng, Q. H. Zhang, X. D. Jia and K. Xi, *J. Colloid Interf. Sci.*, 2014, **418**, 1-7.
9. T. Komatsu and T. Hirose, *Appl. Catal. A-Gen.*, 2004, **276**, 95-102.
10. T. Komatsu, M. Takasaki, K. Ozawa, S. Furukawa and A. Muramatsu, *J. Phys. Chem. C*, 2013, **117**, 10483-10491.
11. W. Y. Song and E. J. M. Hensen, *J. Phys. Chem. C*, 2013, **117**, 7721-7726.
12. M. G. Prakash, R. Mahalakshmy, K. R. Krishnamurthy and B. Viswanathan, *Catal. Sci. Technol.*, 2015, **5**, 3313-3321.
13. N. Pal and A. Bhaumik, *RSC Adv.*, 2015, **5**, 24363-24391.
14. A. Taguchi and F. Schuth, *Micropor. Mesopor. Mat.*, 2005, **77**, 1-45.

15. R. Huirache-Acuna, R. Nava, C. L. Peza-Ledesma, J. Lara-Romero, G. Alonso-Nunez, B. Pawelec and E. M. Rivera-Munoz, *Materials*, 2013, **6**, 4139-4167.
16. B. W. Lu, Y. W. Ju, T. Abe and K. Kawamoto, *RSC Adv.*, 2015, **5**, 56444-56454.
17. X. Y. Liu, A. Q. Wang, X. F. Yang, T. Zhang, C. Y. Mou, D. S. Su and J. Li, *Chem.Mater.*, 2009, **21**, 410-418.
18. Y. Plyuto, J. M. Berquier, C. Jacquiod and C. Ricolleau, *Chem. Commun.*, 1999, 1653-1654.
19. C. P. Mehnert, D. W. Weaver and J. Y. Ying, *J. Am. Chem. Soc.*, 1998, **120**, 12289-12296.
20. J. J. Zhu, T. Wang, X. L. Xu, P. Xiao and J. L. Li, *Appl.Catal. B-Environ.*, 2013, **130**, 197-217.
21. B. Lebeau, C. E. Fowler, S. Mann, C. Farcet, B. Charleux and C. Sanchez, *J. Mater.Chem.*, 2000, **10**, 2105-2108.
22. X. Wei, X. F. Yang, A. Q. Wang, L. Li, X. Y. Liu, T. Zhang, C. Y. Mou and J. Li, *J. Phys. Chem. C*, 2012, **116**, 6222-6232.
23. J. Czaplinska, I. Sobczak and M. Ziolk, *J. Phys. Chem. C*, 2014, **118**, 12796-12810.
24. X. Y. Liu, A. Q. Wang, X. D. Wang, C. Y. Mou and T. Zhang, *Chem. Commun.*, 2008, 3187-3189.
25. C. W. Yen, M. L. Lin, A. Q. Wang, S. A. Chen, J. M. Chen and C. Y. Mou, *J. Phys. Chem. C*, 2009, **113**, 17831-17839.
26. J. W. Allen and J. C. Mikkelsen, *Phys. Rev. B*, 1977, **15**, 2952-2960.
27. G. H. Gao, R. R. Shi, W. Q. Qin, Y. G. Shi, G. F. Xu, G. Z. Qiu and X. H. Liu, *J. Mater. Sci.*, 2010, **45**, 3483-3489.
28. J. Gopalakrishnan, S. Pandey and K. K. Rangan, *Chem. Mater.*, 1997, **9**, 2113-2116.

29. V. N. Kalevaru, A. Benhmid, J. Radnik, M. M. Pohl, U. Bentrup and A. Martin, *J. Catal.*, 2007, **246**, 399-412.
30. P. P. Shanbogh and S. C. Peter, *RSC Adv.*, 2013, **3**, 22887-22890.
31. S. C. Peter, P. P. Shanbogh and U. Subbarao, Patent Application number: WO 2015/011680 A1.
32. T. Aditya, A. Pal and T. Pal, *Chem. Commun.*, 2015, **51**, 9410-9431.
33. D. Makovec, M. Sajko, A. Seisnik and M. Drofenik, *Mater. Chem. Phys.*, 2011, **129**, 83-89.
34. J. Zeng, Q. Zhang, J. Y. Chen and Y. N. Xia, *Nano Lett.*, 2010, **10**, 30-35.
35. S. Sarkar, A. K. Sinha, M. Pradhan, M. Basu, Y. Negishi and T. Pal, *J. Phys. Chem. C*, 2011, **115**, 1659-1673.
36. S. H. Zhang, S. L. Gai, F. He, S. J. Ding, L. Li and P. P. Yang, *Nanoscale*, 2014, **6**, 11181-11188.
37. W. C. Pan, S. H. Zhang, F. He, S. L. Gai, Y. B. Sun and P. P. Yang, *Crystengcomm*, 2015, **17**, 5744-5750.
38. Z. Y. Ji, X. P. Shen, G. X. Zhu, H. Zhou and A. H. Yuan, *J. Mater. Chem.*, 2012, **22**, 3471-3477.
39. Z. F. Jiang, J. M. Xie, D. L. Jiang, J. J. Jing and H. R. Qin, *Crystengcomm*, 2012, **14**, 4601-4611.
40. P. D. Yang, D. Y. Zhao, B. F. Chmelka and G. D. Stucky, *Chem. Mater.*, 1998, **10**, 2033-2038.
41. V. V. Pushkarev, K. J. An, S. Alayoglu, S. K. Beaumont and G. A. Somorjai, *J. Catal.*, 2012, **292**, 64-72.
42. G. C. Bond, M. A. Keane, H. Kral and J. A. Lercher, *Catal. Rev.*, 2000, **42**, 323-383.

43. S. Senapati, S. K. Srivastava, S. B. Singh and H. N. Mishra, *J. Mater. Chem.*, 2012, **22**, 6899-6906.
44. M. Raula, M. H. Rashid, S. Lai, M. Roy and T. K. Mandal, *ACS Appl. Mater. Inter.*, 2012, **4**, 878-889.

## TOC



**Graphical Abstract:** The application of Nickel-Antimony nanoparticles confined in SBA-15 is found to be highly efficient catalyst for the Nitroarene reduction reactions.